UNIVERSITY OF TWENTE.

Investigating 14-3-3's Binding Site upon Interaction with α-Synuclein Through Microscale Thermophoresis Based Competitive Assay

Committee:
Prof. dr. M.M.A.E. Claessens
Dr. C. Blum
Prof. dr. ir. P. Jonkheijm
G. Heesink, MSc

Student:
O.P. Veldman

Faculty of Science and Technology
Department of Nanobiophysics

July 15, 2022

Abstract

Parkinson's Disease (PD) is a neurodegenerative disease characterized by the aggregation of α-synuclein to form toxic multimers in the neuronal cells of the body and brain. It has been shown that the 14-3-3 protein family influences the aggregation of α-synuclein by binding its multimers, preventing misfolding and delaying aggregation. This insight forms opportunities for potential therapeutic approaches regarding the pathogenesis of PD. Here, we performed a competitive assay based on microscale thermophoresis and show that 14-3-3's amphipatic binding pocket may potentially be involved in the interaction between α-synuclein multimers and 14-3-3 proteins.

Abstract

De ziekte van Parkinson (PD) is een degeneratieve aandoening welke wordt gekarakteriseerd door de aggregatie van α-synucleïne tot toxische multimeren in de neuronen van het lichaam en het brein. Onderzoek heeft aangetoond dat de 14-3-3 eiwit familie de aggregatie van α-synucleïne beïnvloed door te binden aan de multimeren, waarmee misvouwing voorkomen wordt en aggregatie wordt vertraagd. Dit inzicht vormt mogelijkheden tot potentiële therapeutische benaderingen met betrekking tot de pathogenese van PD. We hebben een competitief assay uitgevoerd gebaseerd op microscale thermophoresis en laten zien dat 14-3-3's amphipatic binding pocket potentieel betrokken is bij de interactie tussen α-synucleïne multimeren en 14-3-3 eiwitten.

Acknowledgements

I would like to thank prof. dr. Mireille Claessens, dr. Christian Blum, prof. dr. ir. Pascal Jonkheijm and Gobert Heesink, MSc for being part of my Bachelor's committee.

I would like to give special thanks to Gobert Heesink, my daily supervisor who helped me through the course of my research and the experiments involved. Not only did he provide me with all protein stocks, buffers and τ-peptide stocks used in the experiments but he also took the time to answer all my questions, to offer help and useful insights during data analysis and provided extensive and resourceful feedback on my report.

With this, I would also like to thank prof. dr. Mireille Claessens and dr. Christian Blum for offering helpful tips and knowledge during weekly Wednesday meetings and suggesting interesting ideas to investigate during the process of my research.

Lastly, I would like to thank the Nanobiophysics group for offering me the chance to do this Bachelor's Assignment, being able to use the laboratories for my research and for making me feel welcome.

Contents

1 Introduction

Parkinson's Disease (PD) is one of the most common neurodegenerative diseases affecting neurons in the brain [1]. Pathogenesis of Parkinson's Disease is characterised by the accumulation of α-synuclein (α-syn) in so-called Lewy Bodies in the neuronal cells and degeneration of dopaminergic neurons in the substantia nigra pars compacta, an area of the brain involved in movement [2].

α-syn is a 14 kDa intrinsically disordered protein (IDP) abundantly present in the brain, which can exist in different conformations such as monomers, tetramers, oligomers and fibrils [3]. While its exact functions are yet to be determined, it is known to play a role in the release of synaptic vesicles [2]. Natively, α-syn is present as monomers in the presynaptic terminal of neurons with some studies suggesting the occurrence of tetramers as well [1, 4]. However, in patients with PD, α-syn aggregates into toxic oligomers and fibril-like structures (see Figure 1) localized throughout the whole neuronal cell body and its neurites [4, 5]. This indicates that α-synuclein propagates through the cells, possibly hindering cellular function beyond the presynaptic terminal.

Furthermore, it has been shown that the synaptic accumulation of toxic α-syn species results in a decrease of synaptic vesicle fusion and therefore a decrease in neurotransmitter release [2, 4]. This aligns with the degeneration of neurons in the dopamine pathway caused by aggregation of α-synuclein, leading to deficient dopamine release which causes loss of motor control functions characteristic for PD [2].

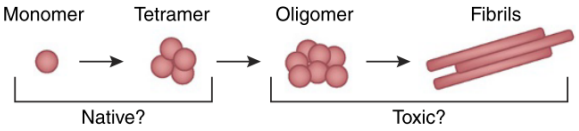

Figure 1: α-synuclein and its different conformations. α-syn is natively found as monomers, with some studies also suggesting the occurrence of α-synuclein as tetramers [6]. In PD, the α-synuclein monomers aggregate to form oligomers (or multimers) and can eventually lead to the formation of fibrils; both conformations which are thought to be toxic [2].

In order to influence and potentially prevent or decrease the aggregation of α-synuclein, it is necessary to gain more insight in how to target α-syn to reduce its toxicity in the cells. Many studies have investigated the role of 14-3-3 in reducing α-syn toxicity and have shown that 14-3-3 binds to α-synuclein multimers, stabilizing them and redirecting the aggregation pathway [7, 8]. 14-3-3 is a family of seven proteins (β, ϵ, γ, η, τ, ζ, σ) present in all eukaryotic cells and play a role in many different activities in the cell such as apoptosis, signal transduction and protein folding and trafficking [7, 9, 10]. Occurring mainly as 56 kDa dimers, 14-3-3 proteins can bind different target proteins in its amphipathic groove. It has been shown that 14-3-3 proteins are present in Lewy Bodies and are known to interact with α-synuclein multimers and other proteins involved in PD, indicating that 14-3-3 does indeed play an important role in the pathology of Parkinson's Disease. This adds to the speculation that 14-3-3 can act as a chaperone to prevent α-syn from misfolding and aggregating [7]. Elevated amounts of 14-3-3 cause it to be in complex with α-syn, thereby preventing

misfolding and aggregation in the cell and stimulating α-syn release [10]. Extracellularly, the formed 14-3-3/α-syn complex prevents uptake and propagation of α-syn by other cells. In neurodegenerative diseases, there is a deficiency of 14-3-3 in and outside the cells, enabling α-synuclein to aggregate and propagate to other neuronal cells [10]. To better understand the exact role of 14-3-3 in reducing the toxicity of α-synuclein, more insight in the interaction between α-syn and 14-3-3 must be provided.

The aim of this research is to investigate 14-3-3's binding sites upon interaction with α-synuclein, specifically looking at 14-3-3τ. This was done through a competition assay based on microscale thermophoresis, measuring the effect of 14-3-3τ on the multimerization of α-synuclein. We investigated the influence of 14-3-3τ on the multimerization alone, and in the presence of a high-affinity peptide which binds in 14-3-3τ's amphipathic groove. Assuming the high-affinity peptide and α-synuclein bind 14-3-3τ in the same groove, the idea was followed that addition of the peptide would show a different effect on the multimerization due to competition.

Competition revealed that 14-3-3τ affects α-syn multimerization. Furthermore, it was seen that the addition of the high-affinity peptide seemingly reversed the effect of 14-3-3τ of the α-syn multimerization, indicating that the amphipathic binding groove may play a role in the interaction between 14-3-3τ and α-synuclein multimers. Other findings suggested possible interaction between the high-affinity peptide and α-syn multimers and capillary surface adherence of the peptide.

1.1 Miscroscale Thermophoresis (MST)

To measure the formation of α-synuclein multimers, the interaction between 14-3-3 and α-synuclein, the interaction between 14-3-3 and the high-affinity peptide and ultimately the competition assay, microscale thermophoresis (MST) was used.

Microscale thermophoresis is a technique with which interaction between two molecules (a target and a ligand) can be measured by following the thermophoretic behaviour of the target molecule upon temperature change. A LED excites the fluorescently labeled molecules (fluorophores), causing a photon to emit which is detected as initial fluorescence. Then, an infrared (IR) laser creates a temperature gradient causing movement of the molecules in solution, also called thermophoresis. Upon binding, the thermophoretic behaviour of the molecules changes and with that, the detected fluorescence [11, 12].

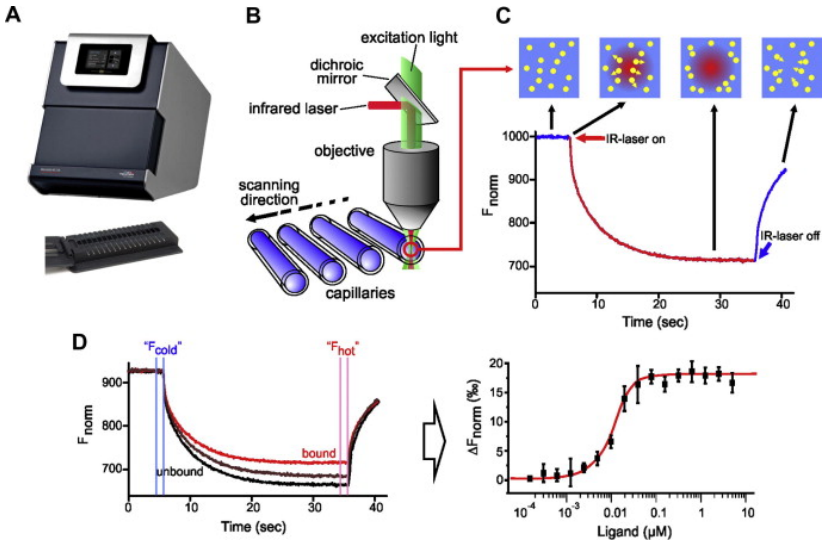

Figure 2: Set up and results of an MST experiment [11]. **(A)** The Monolith NT.115 Blue/Green (NanoTemper Technologies GmbH) instrument. Blue excitation excites photons in the range between 460-480 nm and detects emitted photons between 515-530 nm. Green excitation has an excitation range between 515-525 nm and an emission range between 560-585 nm [12]. **(B)** An infra-red (IR) laser heats the samples, creating a temperature gradient causing movement of fluorescently labeled molecules (thermophoresis) which can be detected. **(C)** Typical TRIC trace of an experiment. Before turning on the IR-laser, an initial fluorescence of the sample is measured. After turning on the laser, changes in fluorescence caused by thermophoresis of the molecules are detected. After 30 seconds, the IR-laser is turned off and the fluorescence signal returns to its initial value due to backdiffusion of the molecules. **(D)** Changes in fluorescence over time caused by the change in thermophoretic behaviour of the molecules can be expressed as the change in normalized fluorescence ($\Delta F_{norm} = \frac{F_{hot}}{F_{cold}} \cdot 1000$). Using an interaction model, binding affinities can be derived.

In MST, the target molecule is fluorescently labeled and kept at constant concentration, whereas the concentration of the unlabeled ligand is varied. Upon binding between target and ligand molecules, the thermophoretic behaviour of the formed complexes in the sample changes, which can be detected as a change in fluorescence. These changes in fluorescence between the bound and unbound complexes as a function of ligand concentration result in so-called TRIC traces (see Figure 2C). These TRIC traces are the result of several occurring processes over a certain time period and can thus be 'divided' into parts (see Figure 3). Initially, the molecules in the sample are equally distributed and during 5 seconds, an initial fluorescence is detected during caused by excitation of the fluorophores induced by the LED (LED_{on}/IR_{off} time or 'initial state'). After this, the IR laser is turned on (LED_{on}/IR_{on} time). Right after the laser is turned on, a change in fluorescence is detected caused by initial heating of the sample (so-called 'T-jump'). After this T-jump, the applied temperature gradient causes movement of the molecules resulting in a further change of detected fluorescence ('Thermophoresis'). After 30 seconds, the IR laser is turned off (LED_{on}/IR_{off} time) and backdiffusion of the molecules causes the fluorescence to go back to its initial value.

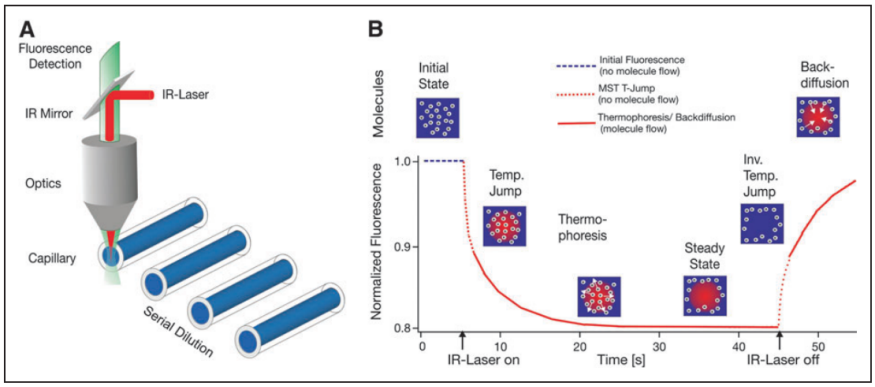

Figure 3: **(A)** A LED excites the fluorophores in the sample, causing fluorescence to be detected. An infrared (IR) laser heats the sample thereby creating a temperature gradient, causing thermophoretic movement of the molecules. **(B)** Occurring processes in the sample during an MST experiment can be separated along the TRIC trace [13].

The change in fluorescence over time as caused by the change in thermophoretic behaviour of the molecules can be expressed as the change in normalized fluorescence (ΔF_{norm}). Plotting this normalized fluorescence as a function of the ligand concentration yields a binding curve. This curve can then be fitted using an interaction model, obtaining binding constants [11].

One of these interaction models is the K_D model, with which the dissociation constant K_D can be determined. This constant K_D is the value of the ligand concentration at which half of the target molecules are bound to the ligand molecules and is given by the formula:

$$K_D = \frac{[P][L]}{[PL]} \tag{1}$$

where [P] is the concentration of the unbound protein (target), [L] the concentration of the unbound ligand and [PL] the concentration of the protein-ligand complex.

The K_D value provides information about the affinity between two proteins. It is advised to use a target concentration no higher than 0.1 times the expected K_D of the interaction [14]. The lower the fitted K_D, the higher the affinity between the two interacting partners [15]. Another measure for affinity between two molecules is the EC_{50}. This EC_{50} value is the ligand concentration at which half of the target is bound and can be derived using the Hill model. The difference between K_D and EC_{50} values is that the K_D is independent of the target concentration, whereas the EC_{50} is not [16]. Thus, which of the fit models to use depends on the nature of the interaction. If the interaction follows a 1:1 stochiometry and is non-cooperative, meaning each target binding site has the same affinity for binding the ligand, the K_D fit should be used. If the interaction does show cooperativity and affinities between target and ligand change upon interaction with each other, the EC_{50} should be used.

In an MST experiment the MST power is the main variable which can be adjusted. Increasing the MST power increases the temperature gradient. A larger induced temperature change usually leads to greater thermophoretic movement of the molecules, which results in a larger change of fluorescence and better resolution of the interaction

[17]. However, an increase in temperature gradient could also lead to temperature-related effects such as unfolding, aggregation or sticking of the protein [18]. Other parameters which can be varied are the LED power and the temperature. Increasing the LED power increases the fluorescence of the sample, but also increases possible photobleaching which expresses the decay of fluorescence [19].

2 Materials and Methods

2.1 Protein Sample Handling

All protein stocks were prepared using a 0.1 mM EDTA, 10 mM NaCl and 10 mM Tris pH 7.4 buffer unless mentioned otherwise.

α-synunclein wild type (α-synWT) and mutant α-syn, with a single alanine to cysteine substitution at residue 140 (α-syn140C), were recombinantly expressed in E. coli B121 (DE3) using the pT7-7-based expression system.

α-synWT stocks were stored at $\pm$200 μM in the above mentioned buffer. α-synAF488 was prepared using α-syn140C. Prior to labeling, α-syn140C was reduced with dithiothreitol (DTT) and then desalted using a Zeba Spin desalting column (Pierce Biotechnology). Then, the mutant α-syn was incubated at room temperature with a molar excess of Alexa Fluor 488 maleimide (Invitrogen). To remove free dye, two desalting steps were done. Resultant labeled protein had a labeling ratio of 1:1 and stocks were stored at 1.1 μM and 11 μM in the aforementioned buffer.

Unlabeled 14-3-3τ was expressed in E. coli and stored at 17.5 μM. 14-3-3τ A647N was prepared by conjugating 14-3-3τ with ATTO 647N NHS-ester (ATTO-TEC GmbH) at a labeling ratio of 1:2. Stocks were prepared in the before mentioned buffer and stored at 10 μM.

14-3-3τ AF568 was prepared by conjugating Alexa Fluor 568 NHS-ester (Invitrogen) with 14-3-3τ at a labeling ratio of 1:7. It should be noted that the Alexa Fluor 568 dye was several years old, resulting in the low labeling ratio. Stocks were prepared in a 100 mM NaCl, 10 mM $MgCl_2$, 2 mM BME and 25 mM HEPES pH 8.0 buffer and stored at 1.8 μM.

τ-peptide was expressed in E. coli and stored at 50 μM and 500 μM. FITC τ-peptide was prepared by conjugating τ-peptide with FITC Isothiocyanate (Invitrogen). Stocks were stored at 10 μM. Both labeled and unlabeled stocks were prepared in HBS.

All labeled and unlabeled protein stocks were flash frozen with liquid nitrogen after preparation and stored at -80 °C.

UV/Vis Absorbance Measurements for Protein Concentrations

To obtain concentrations and label efficiencies of the labeled proteins, the NanoDrop 3300 Fluorospectrometer (Thermo Fisher Scientific) was used. The NanoDrop measures the absorbance of a sample over a full spectrum. To calculate the label efficiency of a labeled protein, the absorbance value of the sample measured at 280 nm (A_{280}) and at the wavelength maximum (A_{max}) of the dye is used. Using Equation 2 and Equation 3, the protein concentration and label efficiency of the dye can then be calculated [20]:

$$\text{protein concentration} = \frac{A_{280} - (A_{max} \times CF)}{\epsilon_{280}} \times \text{dilution factor} \tag{2}$$

$$\text{label efficiency} = \frac{A_{max} \text{ of labeled protein}}{\epsilon_{dye} \times \text{protein concentration}} \times \text{dilution factor} \tag{3}$$

Extinction coefficients, correction factors and wavelength maxima for the used proteins and protein labels are given in Table 1 and Table 2 in *Appendix A*. As mentioned above, α-synWT stocks were ± 200 μM. For 14-3-3τ A647N dye, the label efficiency was 0.45, meaning that each 14-3-3τ dimer roughly had one dye label attached. The 14-3-3τ AF568 revealed a protein concentration of 12.2 μM and a dye concentration of 1.8 μM, resulting in a label efficiency of 0.15. Consequently, the 50 nM 14-3-3τ AF568 target is related to the dye concentration. The corresponding 14-3-3τ protein concentration is then 338 nM. For the unlabeled 14-3-3τ and τ-peptide stocks, no concentration measurements were done.

2.2 MST Measurements

The competition assay and all other interaction experiments were based on microscale thermophoresis. MST experiments were performed by preparing 16 samples. First, 10 μL buffer was added to tubes #2 – #16. Then, 20 μL of the ligand was added to tube 1 (the only empty tube). The 1:1 dilution series was then made by transferring 10 μL from the first tube to the second tube, from the second to the third tube and so on up to the sixteenth tube. After each transfer, the sample was mixed by pipetting up and down. Finally, 10 μL was removed from tube 16 to obtain a total volume of 10 μL in each tube. After the dilution series was made, the target was added. 10 μL of the target was added to each tube, resulting in sixteen 20 μL samples with varying ligand concentration and constant target concentration [21].

All MST experiments were conducted using the Monolith NT.115 Blue/Green (NanoTemper Technologies GmbH). All data were analysed using the MO. Affinity Analysis software. All figures were analyzed by fitting the MST traces over a manually chosen region. The times ranges in this region stretched from -1 second to 0 seconds and from 28.98 to 29.98 seconds (similar to F_{cold} and F_{hot} in Figure 2D). In all MST experiments a 0.1 mM EDTA, 10 mM NaCl and 10 mM Tris pH 7.4 buffer was used for preparation of the samples unless mentioned otherwise. All samples were prepared in Eppendorf Protein LoBind® tubes 0.5 mL and for pipetting the protein solutions, protein low bind tips were used. For the MST measurements, standard capillaries were used. All measurements were – unless mentioned otherwise – measured at 23 °C, 20% LED power and with four MST powers: 20%, 40%, 60% and 80%, which can be seen as respectively green, red, blue and brown colored curves and traces in the figures.

2.2.1 Measuring Protein Interactions between α-Synuclein, 14-3-3τ and τ-Peptide

In order to gain insight in the behaviour of the proteins in the competition assay, four direct interaction experiments were performed using MST as described above. An overview of the measurement specifics discussed below can be found in *Appendix B*.

α-Synuclein Multimerization

14-3-3 is thought to interact with α-syn multimers. To confirm the formation of α-syn multimers from monomers, the interaction between α-synuclein monomers was measured. Samples were prepared containing α-synAF488 as the target at a final

concentration of 50 nM. The ligand consisted of a 1:1 dilution series with α-synWT starting at 112.5 μM down to 3.4 nM. The measurement was performed using blue excitation at 20% LED power.

14-3-3τ Interaction with α-Synuclein
To measure the interaction between 14-3-3τ and α-synuclein, MST was performed using 14-3-3τAF568 as the target at a final concentration of 50 nM. α-synWT was used as the ligand in a 1:1 dilution series starting at a concentration of 112.5 μM down to 3.4 nM. MST was then performed, using green excitation at 20% LED power. This same interaction was also performed using 14-3-3τ at a different concentration labeled with a different dye, namely ATTO 647N. See *Investigating Different Target Behaviour upon Interaction with α-Synuclein Ligand* for details on that experiment.

14-3-3τ Interaction with τ-Peptide
The τ-peptide is a small, 30 amino acid peptide with known high affinity[1] to 14-3-3τ. For MST, the target was 50 nM 14-3-3τ AF568 and τ-peptide was used as ligand starting from 10 μM down to 0.31 nM.

τ-Peptide Interaction with α-Synuclein
The interaction between the τ-peptide and α-synuclein was also measured. 200 nM FITC labeled τ-peptide was added as a target to a 1:1 ligand dilution series of α-synWT ranging from 110 μM to 3.4 nM.

2.2.2 Competitive Assay (based on α-synuclein multimerization)

The competition experiment looked at the influence of adding 14-3-3τ and a bivalenty phoshorylated peptide derived from the τ-protein (further referred to as τ-peptide) on the multimerization of α-synuclein. For all experiments in the competition assay, 50 nM α-synAF488 was used as the labeled target and α-synuclein wild type as the ligand, such that the multimerization was identical in each experiment. To measure their effect on the multimerization of α-syn, 14-3-3τ and τ-peptide were added at varying constant concentrations. In total, three sets of experiments were conducted with each measuring different 14-3-3τ and τ-peptide concentrations. The experiment sets measured the multimerization of α-synuclein in the absence of both 14-3-3τ and the τ-peptide (experiment i), in presence of only 14-3-3τ (experiment ii) and in presence of both 14-3-3τ and the τ-peptide at two different concentrations (experiment iii).

Experiment set 1
Experiment (i) measured the the multimerization of α-synuclein by mixing 50 nM of α-synAF488 target with a ligand dilution series of α-synWT. Experiment (ii) was measured by again mixing 50 nM α-synAF488 target with a ligand dilution series of α-synWT, this time also adding 338 nM 14-3-3τ. Samples for experiment (iii) were prepared in the same way, this time adding not only 338 nM 14-3-3τ but also τ-peptide at a final concentration of 338 nM to the α-syn multimers. At this concentration of τ-peptide, a fraction of 0.47 of 14-3-3τ would be bound to the peptide.

Experiment set 2
Experiment (ii) was done at a 14-3-3τ concentration of 750 nM. Experiment (iii) was

[1]Researchers have measured an affinity of 20-200 nM, but it has not yet been officially reported.

measured at two different τ-peptide concentrations. These peptide concentrations were based on the expected fraction of 14-3-3τ which would then be bound to the τ-peptide. We looked at the difference in interaction when approximately half of the 14-3-3τ was bound to the τ-peptide (f_{bound}=0.5) and when almost all of the 14-3-3τ was bound the τ-peptide (f_{bound}=0.95). Using Equation 1 and given the total protein and ligand concentrations $[P]_t$ = [P] + [PL] and $[L]_t$ = [L] + [PL], the expected concentration of the τ-peptide at which f_{bound}=0.5 and f_{bound}=0.95 could be calculated (see table below).

fraction bound	K_D (nM)	[P] (nM)	[L] (nM)
0.5	$K_D = 200$	750	575
0.95	$K_D = 200$	750	4512

with [P] = concentration 14-3-3τ and [L] = concentration τ-peptide.

This resulted in one series of samples measuring the multimerization of α-syn with 750 nM 14-3-3τ and 575 nM τ-peptide added, and a second series of samples measuring the same multimerization but with 750 nM 14-3-3τ and 4.5 μM τ-peptide added.

Experiment set 3
The last set of experiments had the same outline as experiment set 2, this time using 1.5 μM 14-3-3τ in both experiments (ii) and (iii). This gave the two concentrations of τ-peptide to be added for the different bound fractions as seen below.

fraction bound	K_D (nM)	[P] (nM)	[L] (nM)
0.5	$K_D = 200$	1.5	950
0.95	$K_D = 200$	1.5	5200

This resulted in a series of samples measuring the multimerization of α-syn with 1.5 μM 14-3-3τ and 950 nM τ-peptide added, and a second series of samples measuring the same multimerization but with 1.5 μM 14-3-3τ and 5.2 μM τ-peptide added.

3 Investigating Different Target Behaviour upon Interaction with α-Synuclein Ligand

During protein interaction experiments, we encountered several issues regarding protein behaviour in MST, such as irregular TRIC traces, sample inhomogeneities, possible temperature induced effects, changes in initial fluorescence and surface adherence of the target. Here, we describe how these issues were overcome and used to optimize the experimental design and setup to eventually obtain the final results as discussed in *Results and Discussion*.

3.1 Multimerization Measurement of α-Synuclein

The starting point of all experiments and ultimately the competition assay, is that α-synuclein forms multimers. Thus, it is important that the multimerization occurring in the experiments is reliable by validating the results.

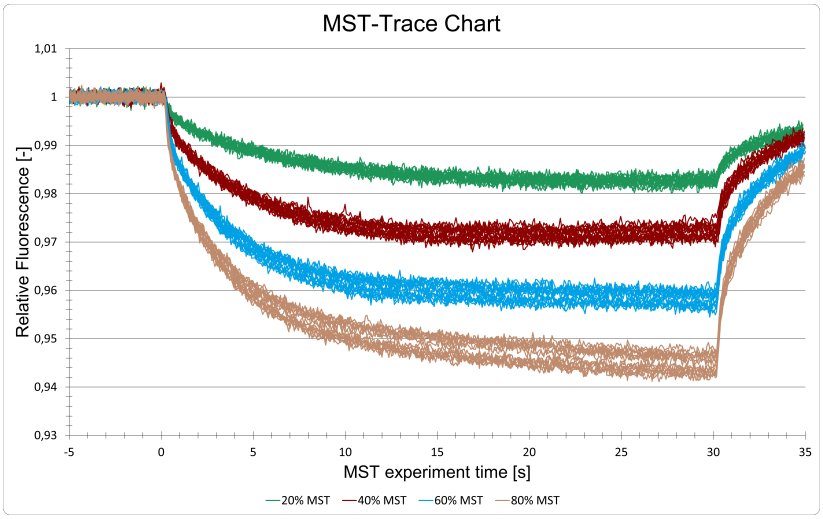

(a)

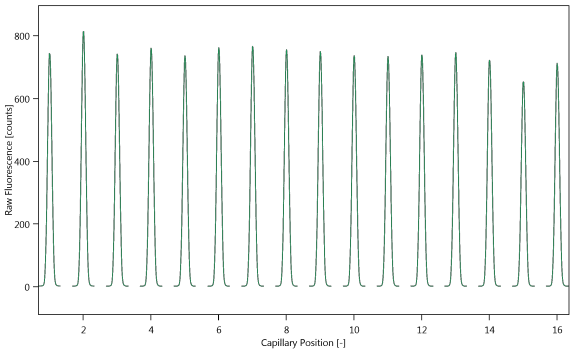

(b) Capillary scan

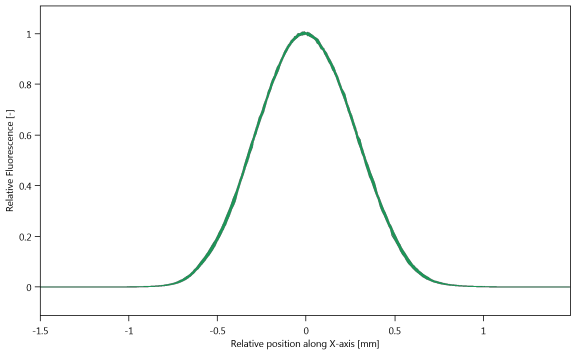

(c) Capillary shape

Figure 4: Normalized TRIC traces and capillary scans and shapes of the α-synuclein multimerization. **(a)** Observed TRIC traces follow 'typical' trace. Green, red, blue and brown curves correspond to 20%, 40%, 60% and 80% MST power, respectively. **(b)** Initial fluorescence shows around 780 counts with small fluctuations between capillaries. **(c)** Capillary shape shows identical smooth shape for all capillaries with no indications of target sticking.

As Figure 4 shows, measured TRIC traces nicely follow the 'typical' trace and

the capillary scan is smooth and identical for all measured capillaries. The initial fluorescence shows consistent values with little fluctuations, all within 10% margin. Furthermore, we observed no strange effects or irregularities as the ones mentioned above, concluding that we can rely on the validity of the obtained multimerization curves which will be used in the competition assays.

3.2 Behaviour of Differently Labeled 14-3-3τ Targets

14-3-3τ ATTO 647N Sample Inhomogeneity

The first experiments measuring potential interaction between 14-3-3τ and α-synuclein were performed at 37 °C with 14-3-3τ labeled with ATTO 647N dye. The target was 1 μM 14-3-3τ A647N in a α-syn ligand series ranging from 112.5 μM to 13.7 nM. This much higher target concentration as opposed to the 50 nM 14-3-3τ AF568 target is due to the characteristics of the label. The A647N label is further away from the excitation range of the Monolith NanoTemper and thus higher target concentrations are required to reach similar initial fluorescence counts as with the AF568 label. Figure 5 shows the TRIC traces of the experiment, comparing two identical measurements performed only a few days apart. The second experiment (Figure 5b) shows many bumps along the trace as opposed to the first experiment (Figure 5a). To see whether the observed roughness was caused by either 14-3-3τ or the α-syn ligand, we performed a similar experiment measuring the target 14-3-3τ A647N alone. Results showed the same bumps along the traces (data not shown). In combination with the absence of these rough TRIC traces in the α-syn multimerization measurement, this indicated that 14-3-3τ was causing a problem.

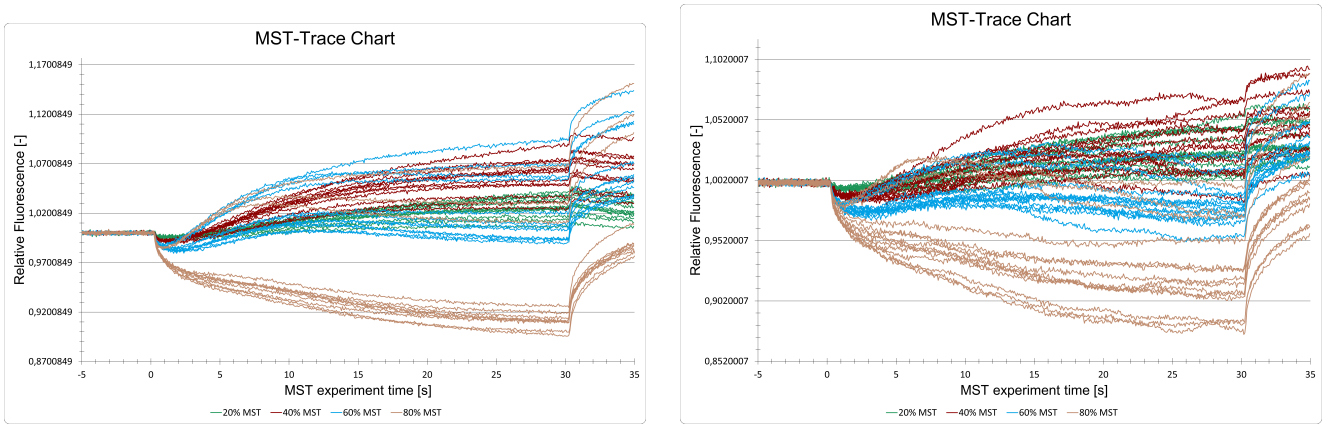

(a) Experiment set 1: 14-3-3τ A647N with α-synWT.

(b) Experiment set 2: 14-3-3τ A647N with α-synWT.

Figure 5: Normalized TRIC traces of 14-3-3τ A647N with α-synWT measured at 37 °C. Target concentration was 1 μM and ligand concentration started at 112.5 μM down to 13.7 nM. Both sets shows identical experiments only performed a few days apart. Green, red, blue and brown traces correspond to 20%, 40%, 60% and 80% MST power, respectively.

After repeatedly observing bumps along the MST traces, a new batch of 14-3-3τ A647N was prepared. However, the MST traces again showed bumps along the trace as seen in Figure 6a. Bumps and irregularities along a MST time trace indicate the presence of aggregates in the sample, corresponding to the movement of larger formed particles in and out of the detected sample volume [18]. Presence of aggregates greatly hinders sample homogeneity, thereby influencing the MST data negatively. To ensure

homogeneity of the target sample, all target stocks were centrifuged for 10 minutes at 20,000g at 4 °C, as advised by NanoTemper [21], prior to sample preparation. Centrifuging the target sample ensures that potentially formed aggregates are pushed to the bottom of the sample, after which the supernatant can be used for sample preparation. This added centrifuging step resulted in smoother MST traces without bumps (see Figure 6b).

However, pushing down aggregates in the solution results in a lower target concentration of the supernatant. Nevertheless, this seemed not to be much of a problem considering the 14-3-3τ target concentration was somewhat in the high range. A target concentration set at 1 μM would mean that K_D values of 10 μM would be expected, which is much higher than expected values.

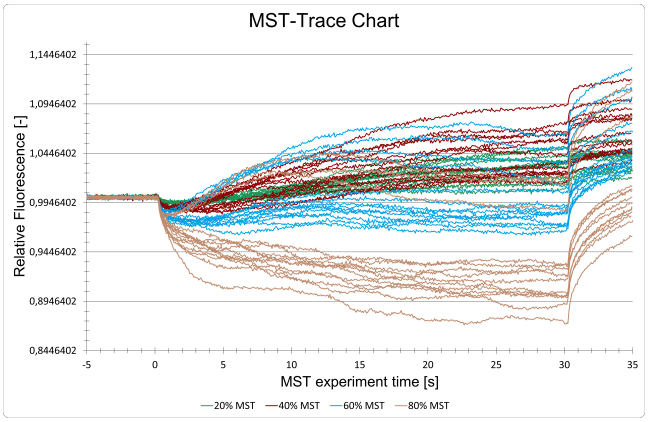

(a) 14-3-3τ A647N with α-synWT at 37 °C without centrifugation.

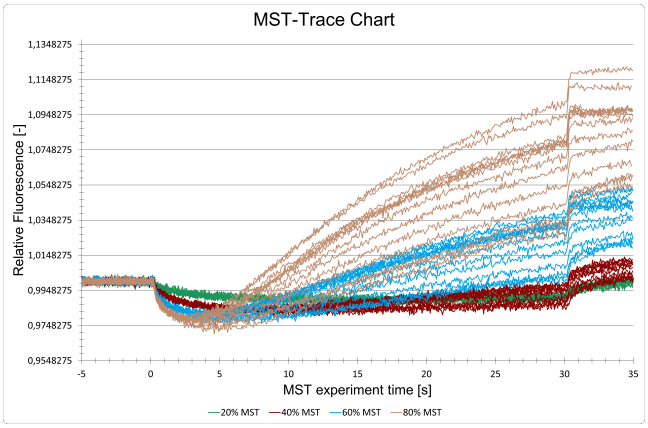

(b) 14-3-3τ A647N with α-synWT at 23 °C after centrifugation.

Figure 6: Normalized TRIC traces of 14-3-3τ A647N with α-synWT. Target concentration was 1 μM and ligand concentration started at 112.5 μM down to 13.7 nM. Green, red, blue and brown traces correspond to 20%, 40%, 60% and 80% MST power, respectively. It can be seen that the TRIC traces continuously increase, indicating unfolding of the protein. This effect seems to be irreversible, because the fluorescence does not go back to its initial value after turning off the IR laser (see trace between 30 and 35 seconds).

Another important note is that Figure 6 not only compares two measurements with and without the extra centrifuging step, but both measurements were performed at different temperatures (respectively 37 °C and 23 °C). Thus, one could argue that the previously observed bumps were due to the higher temperature and not due to lack of centrifugation. Therefore, we also measured 14-3-3τ A647N alone at 23 °C without centrifuging the target. Results again showed rough TRIC traces (data not shown), indicating bumps along the traces were not caused by an increased temperature.

14-3-3τ A647N Label Limitations and Temperature Dependent Effects

As shown in both Figure 5 and Figure 6, the TRIC trace increases over time instead of following the typical MST trace as seen with the multimerization, especially at higher MST powers (60%, 80%). Additionally, though the traces of both experiments in Figure 6 display this behaviour of increasing TRIC trace, this behaviour is not consistent between measurements. It seems that the change in thermophoretic behaviour of the molecules in solution results in greater fluorescence. Similar effects have been discussed in literature, suggesting this might be due to irreversible temperature induced effects such as unfolding of the protein [18]. The irreversibility effect is indicated by

a continuous increasing TRIC trace, even after turning off the IR laser. Though it seemed unlikely that the induced temperature gradient of the Monolith NanoTemper would exceed the melting temperature of the protein, it was reported that the temperature gradient can increase above 10K at higher MST powers (>40%) [18]. Thus, to minimize these potential temperature induced effects, it was decided to conduct further experiments at 23 °C instead of 37 °C from the previous experiments. However, as Figure 6b shows, the increase in relative fluorescence was still observed even at 23 °C.

14-3-3τ A647N Target Sticking

Further look at the capillary shape revealed an uneven capillary shape between different ligand concentrations. A closer look at the capillary shape depicted in Figure 7 revealed a wider capillary shape at lower ligand concentrations. In contrast, higher ligand concentrations revealed more narrow capillary shapes. Literature describes this effect as the result of possible target sticking to the capillary surface [18]. At lower ligand concentrations, the target will stick to the capillary surface, resulting in a wider capillary shape. On the contrary, at higher ligand concentrations the surface will become saturated with the ligand therefore preventing target sticking, which results in the more narrow shape observed.

Taking into account all the observed issues with ATTO 647N as the target label, being unlikely unfolding of the protein at low temperature, differences in homogeneity between target batches and the possibility of target adsorption, it was decided to label 14-3-3τ with a different dye, namely Alexa Fluor 568.

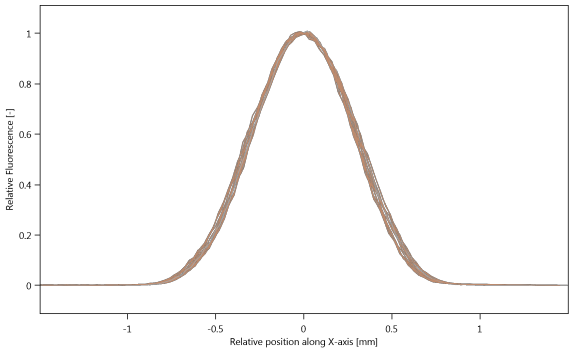

Figure 7: Capillary shape of measurement with 14-3-3τ A647N and α-synWT. Target concentration was 1 μM with ligand concentration ranging from 112.5 μM to 13.4 nM.

MST traces of the newly labeled 14-3-3τ target with α-synWT ligand are shown in Figure 8. The traces show the expected 'typical' MST traces with no bumps, indicating there was no issue of aggregates in the target sample anymore. Thus, for further experiments regarding protein interactions using 14-3-3τ as the target, 14-3-3τ AF568 was used. It was found that for 14-3-3τ AF568 the extra centrifugation step was unnecessary and thus, to maintain target concentration, no centrifugation was performed. All measurements were performed at 23 °C.

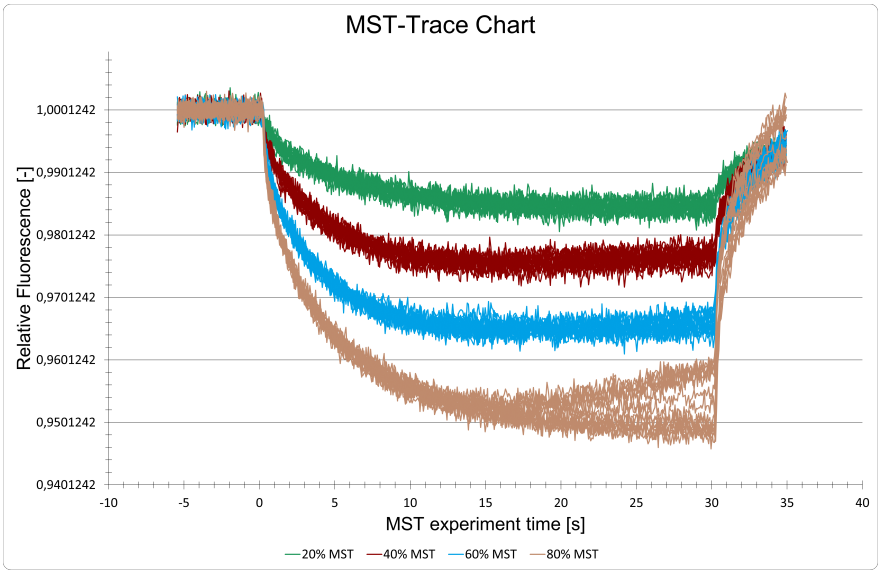

(a)

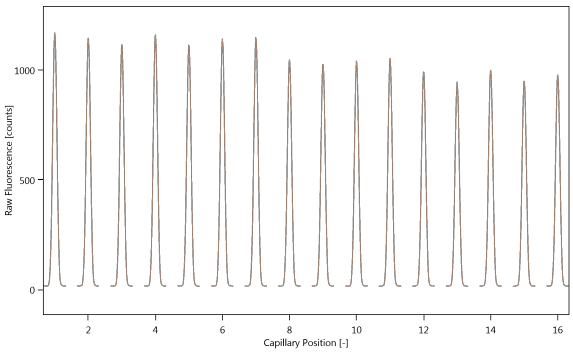

(b) Capillary scan

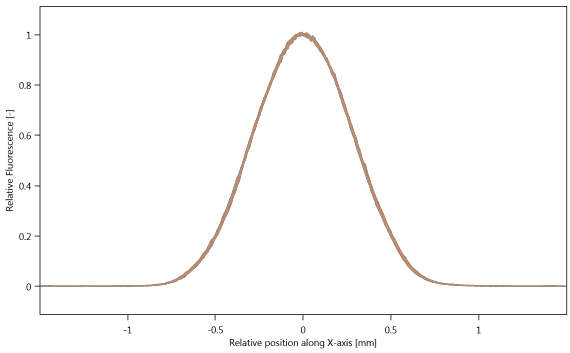

(c) Capillary shape

Figure 8: Normalized TRIC traces and capillary scans and shapes from the measurement with 14-3-3τ AF568 and α-synuclein. **(a)** TRIC traces of 14-3-3τ AF568 with α-synWT at 23 °C. Target concentration was 50 nM and ligand concentration started at 112.5 μM down to 3.4 nM. Green, red, blue and brown curves correspond to 20%, 40%, 60% and 80% MST power, respectively. **(b)** Initial fluorescence shows around 1100 counts with fluctuations between capillaries within a 10% margin. **(c)** Capillary shape shows identical smooth shape for all capillaries with no indications of target sticking.

3.3 Behaviour of the FITC Labeled τ-Peptide

When measuring the possible interaction of the τ-FITC labeled peptide with α-synuclein, several behavioural effects of the target were observed. TRIC traces are shown in Figure 9a, revealing typical smooth traces. However, it can be seen that photobleaching has occurred. This is not completely unexpected, since the FITC label is prone to high rates of photobleaching [22]. As depicted in Figure 9b, the initial fluorescence of the samples shows an increase as the ligand concentration increases. This can be the result of loss of material, as caused by sticking, during sample preparation [21]. Target adsorption can also be seen by analyzing the capillary shape. In the case of adhesion of the target to the capillary surface, this can be seen by a change in capillary shape as the ligand concentration increases, as was previously discussed. As shown in Figure 9c, the capillary shapes become more narrow for higher ligand concentrations. However, the typical 'dipped' peak which is also characteristic for target sticking was not observed.

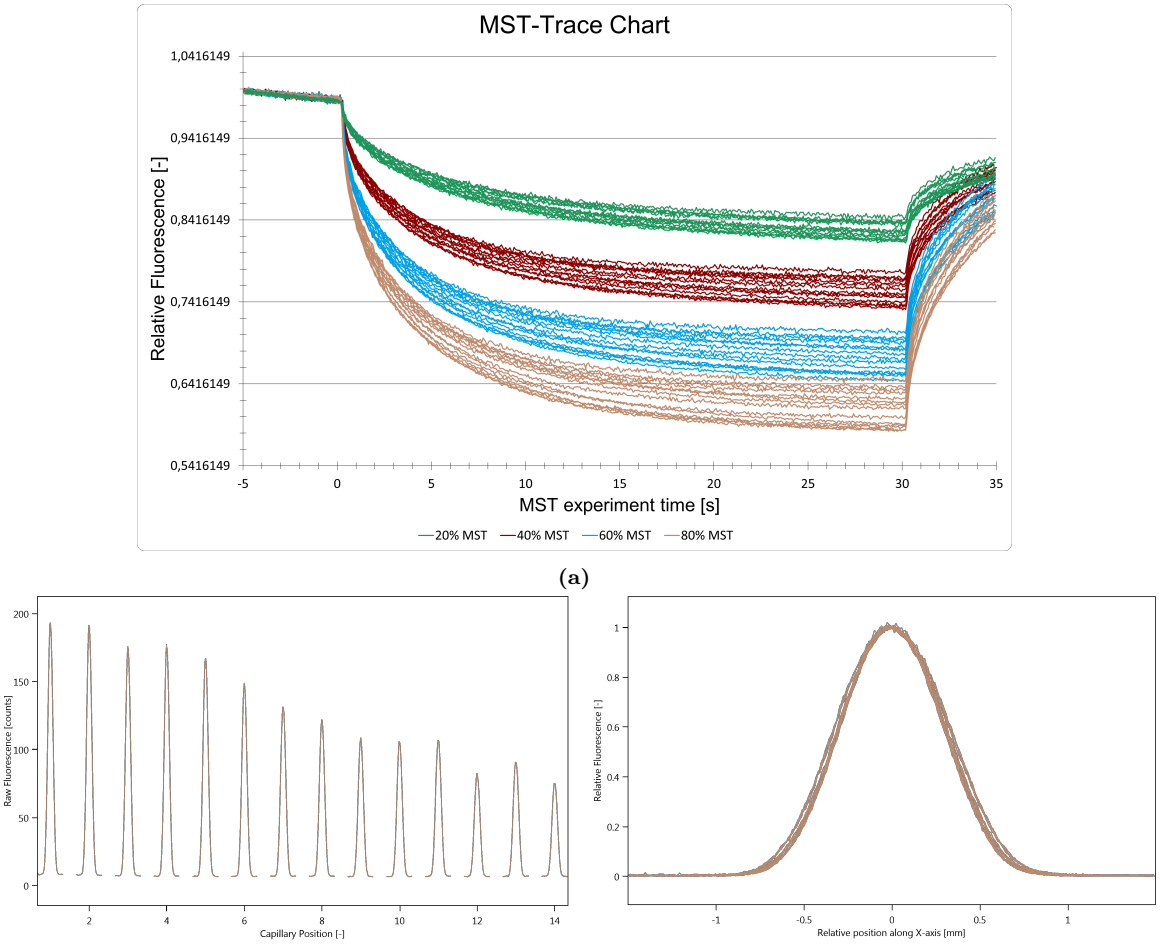

(a)

(b) Capillary scan

(c) Capillary shape

Figure 9: Normalized TRIC traces and capillary scans and shapes from the interaction between the FITC-labeled τ-peptide and α-synuclein. **(a)** Observed TRIC traces follow 'typical' MST trace. In the region between -5 and 0 seconds, the photobleaching effect can be observed by a decrease in relative fluorescence. **(b)** Initial fluorescence increases upon increasing ligand concentration (from right to left). **(c)** Capillary shape shows increasing narrow shape for higher ligand concentrations, indicating target sticking. Shape does follow typical shape without irregular, dipped peaks.

One could argue that a different dye label could form a possible solution to the effects observed, as with the 14-3-3τ. However, the FITC-τ peptide is the only labeled τ-peptide we have available, canceling out this possible solution. When investigating other peptides, a different use of label could be taken into account.

4 Results and Discussion

The results obtained from the experiments showed seemingly contradicting results. Therefore, we will discuss the results from different perspectives giving different explanations for the contradicting results.

4.1 α-Synuclein Multimerization

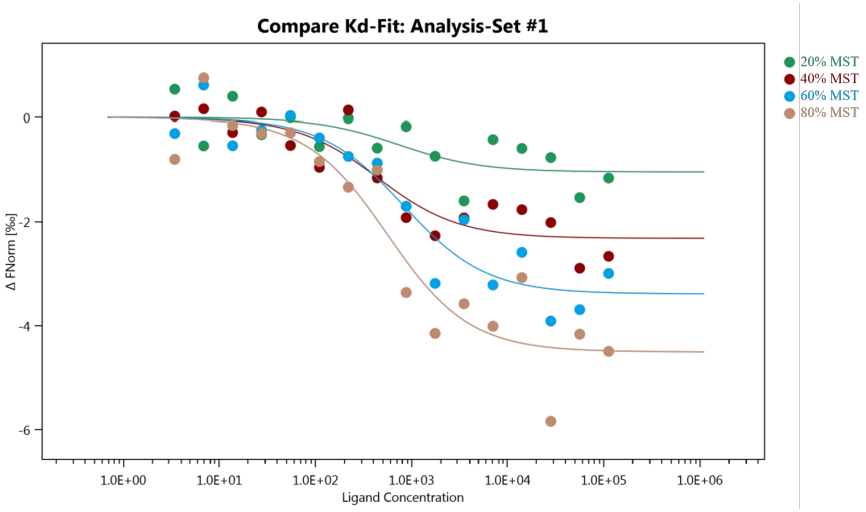

(a)

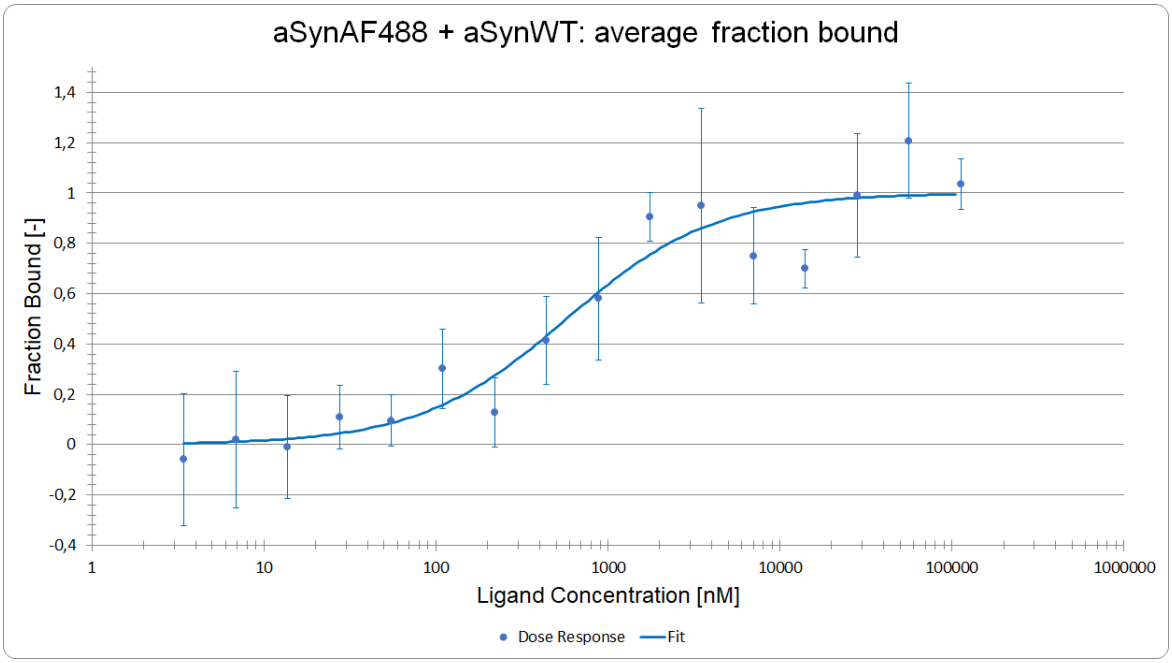

(b)

Figure 10: (a) Normalized binding curves of the multimerization of α-synuclein monomers using the K_D fit model. Target concentration was 50 nM α-synAF488. Ligand concentration was a 1:1 dilution series starting at 112.5 μM down to 3.4 nM α-synWT. Ligand concentrations are given in nM on a logarithmic x-axis. Measurement done at 23 °C. **(b)** Average normalized fraction bound curve of the multimerization. Corresponding average K_D = 564.4 ± 397.0 nM. Error bars correspond to the standard deviation from the averaged four MST power measurements.

Figure 10 shows the normalized binding curves of the multimerization of α-synuclein monomers in an MST experiment performed at 23 °C. Figure 10b shows the average of the four normalized fraction bound curves of the multimerization. The curve was fitted with the K_D model, yielding $K_D = 564.4 \pm 397.0$ nM. Replicate measurements showed reproducible results, affirming the multimerization to be a good system of study to observe changes upon addition of 14-3-3τ and τ-peptide. It can be seen that higher MST powers seem to have a stronger effect on the interaction and induce a larger dose response.

4.2 Interaction between 14-3-3τ and α-Synuclein

Performing MST with 50 nM 14-3-3τ AF568 as the target and α-syn as the ligand yielded the binding curves as shown in Figure 12. Fitted K_D values are shown in Figure 11c. Interaction of 14-3-3τ AF568 with α-synuclein revealed no apparent binding curve. Only at high MST powers of 70%, 80% and 90% binding curves could be fitted. Averaging the normalized fraction bound curve of the interaction at high MST powers yields an average fitted K_D of 441.5 ± 317.2 nM.

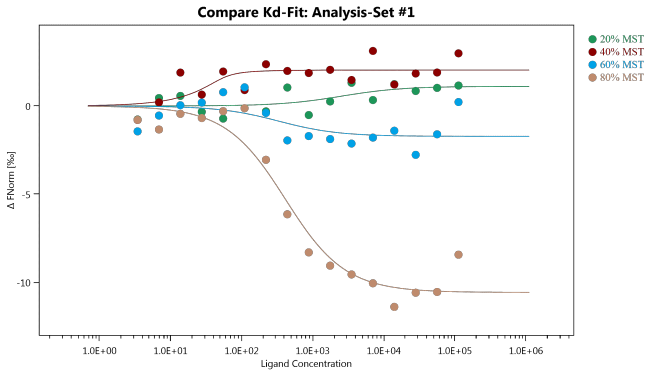

(a)

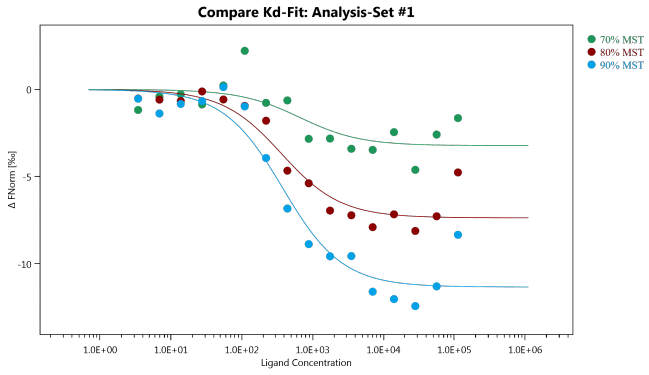

(b)

(c) Fitted K_D values.

MST power	K_D [nM]
20%	2174.3 ± 3900.3
40%	4.4 ± 13.7
60%	309.0 ± 546.9
70%	630.83 ± 697.22
80%	340.09 ± 132.29
90%	352.8 ± 352.83

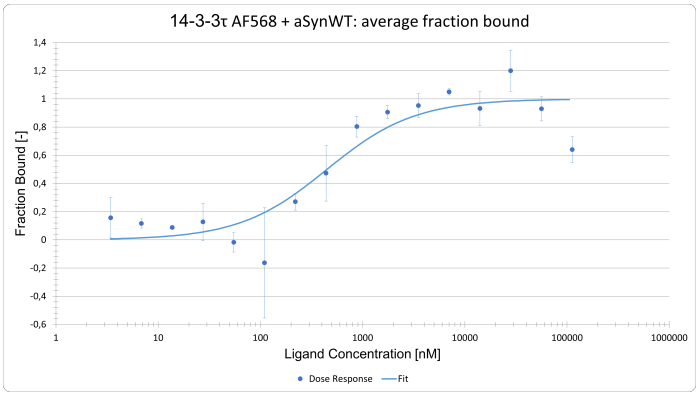

(d)

Figure 12: Normalized binding curves of the interaction between 14-3-3τ and α-synuclein using the K_D fit model. **(a)** Normalized binding curves of the interaction at MST powers 20%, 40%, 60% and 80% show no binding at lower MST powers. **(b)** Normalized binding curves of interaction at higher MST powers (70%, 80% and 90%). **(d)** Average fraction bound curve of the interaction between 14-3-3τ AF568 and aSynWT at high MST powers of 70%, 80% and 90% (average fitted $K_D = 441.5 \pm 317.2$ nM). Target concentration was 50 nM 14-3-3τ AF568. Ligand concentration was a 1:1 dilution series starting at 112.5 μM down to 3.4 nM α-synWT. Ligand concentrations are given in nM on a logarithmic x-axis. Measurement done at 23 °C.

Figure 11d and the average fitted K_D of 441.5 ± 317.2 nM shows that 14-3-3τ does appear to interact with α-synuclein. Higher MST powers generate a larger temperature gradient, resulting in an increase in thermophoretic behaviour of the molecules and therefore a higher dose response. However, with interactions also being affected by temperature, different MST powers can also exert a different effect on the interaction. It should be noted that higher MST power could also cause unwanted effects such as aggregation or unfolding of the sample as well as photobleaching, so the choice of MST power should be considered carefully [18]. However, the presence of aggregates, unfolded species and the photobleaching effect in the sample can be visualised in the observed TRIC traces as respectively bumps and a continuous decrease in initial fluorescence, as mentioned in *Investigating Different Target Behaviour upon Interaction with α-Synuclein Ligand*. The TRIC traces of this interaction showed neither of these effects along the trace (data not shown), promoting the reliability of the observed binding curves.

4.3 Interaction between 14-3-3τ and τ-Peptide

Interaction measurement of 14-3-3τ AF568 and the τ-peptide revealed no binding curve whatsoever, as shown in Figure 14, despite the high known affinity between the two proteins. The τ-peptide is a small peptide binding to a large 14-3-3τ dimer. Upon binding of the small τ-peptide ligand, thermophoretic behaviour of the 14-3-3τ AF568/τ-peptide complex is not changed drastically compared to the thermophoretic behaviour of the unbound 14-3-3τ target. Thus, detected change in fluorescence upon binding to the ligand would not be sufficient to fit a binding curve due to this small contrast in changed fluorescence. To obtain binding curves of the interaction between 14-3-3τ and the τ-peptide, the τ-peptide should be taken as the labeled target at a constant concentration with unlabeled 14-3-3τ as the ligand in a serial dilution. Changes in fluorescence of the smaller target would be detected and binding could be measured. However, for further measurement purposes, it was assumed that the peptide does indeed bind to 14-3-3τ with high affinity.

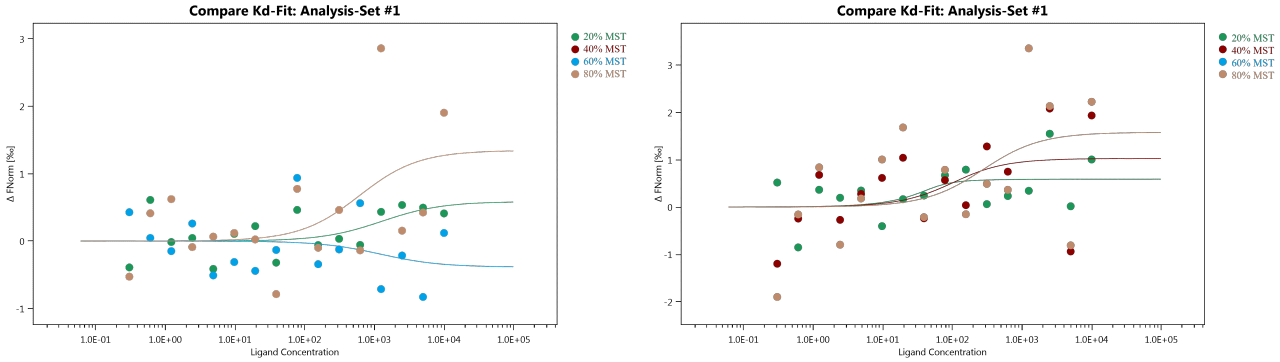

(a) **(b)**

Figure 14: Normalized curves of the interaction of 14-3-3τ and τ-peptide using the K_D fit model show no binding between 14-3-3τ and τ-peptide. Target concentration was 50 nM 14-3-3τ AF568. Ligand concentration was a 1:1 dilution series starting at 112.5 μM down to 3.4 nM τ-peptide. Ligand concentrations are given in nM on a logarithmic x-axis. Curve at 40% MST power failed to plot. Measurement done at 23 °C. Binding curves are fitted in the 'Thermophoresis' region **(a)** and in the 'Manual' region **(b)**. Green, blue, red and brown curves correspond to 20%, 40%, 60% and 80$ MST power, respectively.

4.4 Interaction between τ-Peptide and α-Synuclein

Measurement of the interaction between the FITC labeled τ-peptide and α-synuclein showed interaction to an extent. At 95% LED power, initial fluorescence counts of around 180 were detected (see Figure 9b), which is below the minimum 200 counts as advised by NanoTemper [21]. This could be caused by a low labeling efficiency, loss of material or photobleaching as a result of the high LED power [12], with the FITC label known to be sensitive to the latter [22]. Moreover, NanoTemper states that if the K_D of an interaction is lower than the target concentration, fluorescence counts of 200 can be expected at 95% LED power [21]. Looking at the average fitted K_D of 166.8 $\pm$ 201.9 nM, which is lower than the 200 nM target concentration, these low fluorescence counts would then have been expected.

Looking at Figure 15, one could argue that two plateaus have formed and that there is binding occurring with an average fitted K_D of 166.8 $\pm$ 201.9 nM. The experiment was measured with 14 samples, therefore missing two extra points from the plateau at the lowest ligand concentrations. The fitted binding curve could also be the result of target sticking to the capillary surface as seen in Figure 9c. At lower concentrations, the τ-peptide adheres to the surface of the capillary, resulting in a low measured fluorescence. As the concentration α-synWT increases, the capillary surface is saturated by the ligand thereby decreasing stickiness of the τ-peptide and increasing the detected fluorescence. This phenomenon could cause a false positive binding curve. While it is difficult to say if α-synuclein binds to the τ-peptide with a certain affinity, it should be noted that a certain effect is visible which would require further research.

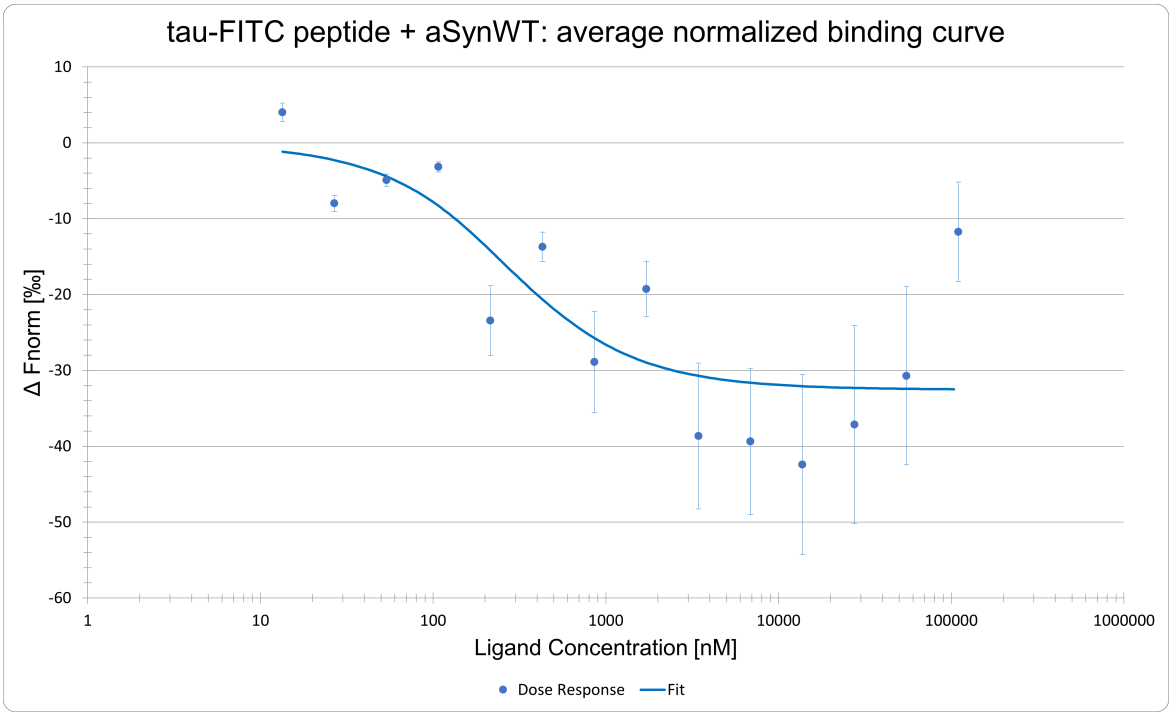

Figure 15: Average normalized binding curve of the interaction between the τ-peptide and α-synuclein (fitted $K_D = 166.8 \pm 201.9$ nM). Target concentration was 200 nM τ-FITC peptide. Ligand concentration was a 1:1 dilution series starting at 110 μM down to 13.4 nM. Ligand concentrations are given in nM on a logarithmic x-axis. Measurement done at 23 °C with 95% LED power. Error bars correspond to the standard deviation from the averaged four MST power measurements.

4.5 Competitive Assay with α-Synuclein, 14-3-3τ and τ-Peptide

Measurements of the competition assays revealed varying contradictory results, which will be discussed from different perspectives.

Experiment 1

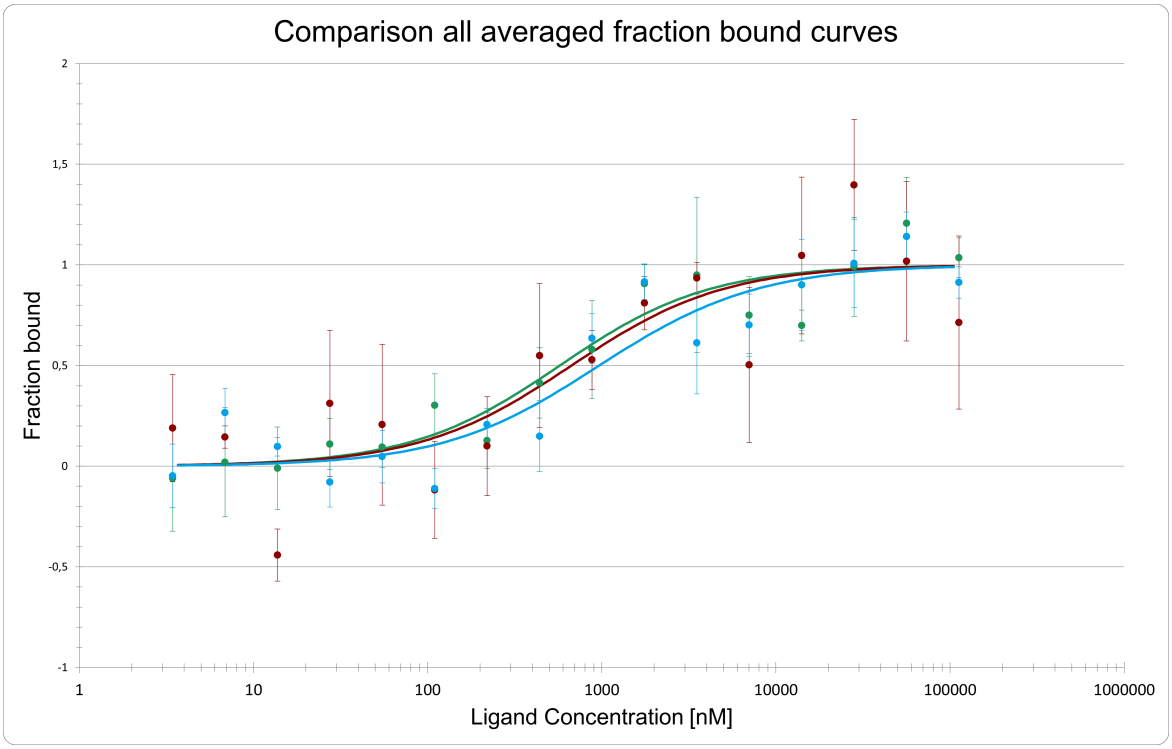

Figure 16: Average fraction bound curves of different protein interaction measurements. The green curve shows α-syn multimerization (fitted K_D = 564.4 ± 397.0 nM). The red curve shows α-syn multimerization in presence of 338 nM 14-3-3τ (fitted K_D = 679.8 ± 877.5 nM). The blue curve shows α-syn multimerization in presence of 338 nM 14-3-3τ and 338 nM τ-peptide (fitted K_D = 1085.7 ± 815.6 nM). Target concentration α-synAF488 was 50 nM. Ligand concentration α-synWT ranges from 112.5 μM down to 3.4 nM. Curves are average of the fraction bound curves at 20%, 40%, 60% and 80% MST power. Ligand concentrations are given in nM on a logarithmic x-axis. Measurement done at 23 °C. Error bars correspond to the standard deviation from the averaged four MST power measurements.

The multimerization of α-syn can be fitted into a binding curve depicted in green, using the K_D model yielding a fitted K_D of 564.4 ± 397.0 nM. Addition of 338 nM 14-3-3τ Figure 16 shows a slight shift to the right of the binding curve (red curve) with corresponding fitted K_D = 679.8 ± 877.5 nM. After also adding 338 nM τ-peptide, a further shift to the right is shown by the blue curve (fitted K_D = 1085.7 ± 815.6 nM). Data points show a relatively large error.

Experiment 2

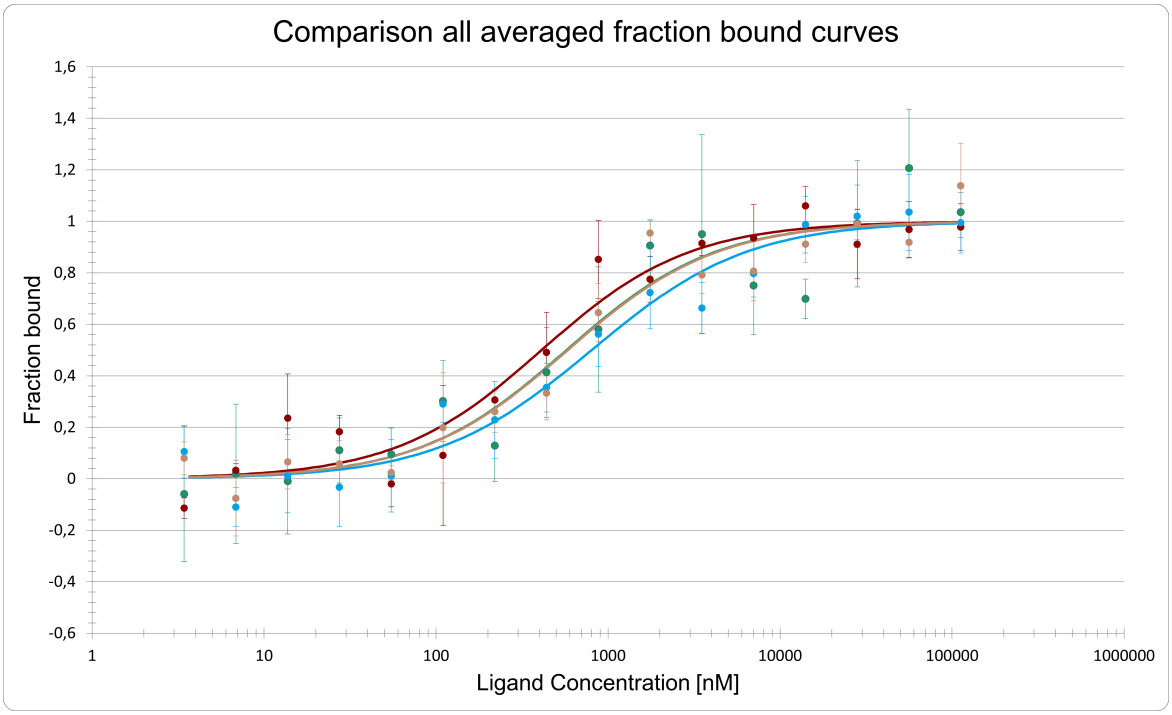

Figure 17: Average fraction bound curves of different protein interaction measurements. The green curve shows α-syn multimerization (fitted K_D = 564.4 ± 397.0 nM). The red curve shows α-syn multimerization in presence of 750 nM 14-3-3τ (fitted K_D = 401.0 ± 187.6 nM). The blue curve shows α-syn multimerization in presence of 750 nM 14-3-3τ and 575 nM τ-peptide (fitted K_D = 871.4 ± 403.0 nM). The brown curve shows α-syn multimerization in presence of 750 nM 14-3-3τ and 4.5 μM τ-peptide (fitted K_D = 567.4 ± 262.4 nM). Target concentration α-synAF488 was 50 nM. Ligand concentration ranged from 112.5 μM down to 3.4 nM. Curves are average of the fraction bound curves at 20%, 40%, 60% and 80% MST power. Ligand concentrations are given in nM on a logarithmic x-axis. Measurement done at 23 °C. Error bars correspond to the standard deviation from the averaged four MST power measurements.

Addition of 750 nM 14-3-3τ to α-synuclein shows a left shift compared to the multimerization curve of α-synuclein depicted in green (see Figure 17), indicating that multimerization occurs at lower concentrations. This is in accordance with the expectation that 14-3-3τ binds to α-syn multimers. Upon interaction with 14-3-3τ, the equilibrium of multimerization shifts towards the side of multimer formation. This can be interpreted as multimers being more easily formed, resulting in the left shift as depicted.

The competition measurement with 750 nM 14-3-3τ shows no change in binding curve at the higher 4.5 μM concentration of added τ-peptide. Since 14-3-3τ is know to bind the τ-peptide in its amphipathic binding groove, this observation indicates that this amphipathic groove may indeed play a role in the binding of α-synuclein. Namely, at the higher concentration of peptide nearly all of the 14-3-3τ is expected to be bound to the peptide, thus occupying 14-3-3τ's amphipathic groove. Assuming α-syn binds to 14-3-3τ in this same groove, this would make it more difficult for α-synuclein to compete for its binding. Thus, if α-syn is unable to bind to 14-3-3τ, the resultant binding curve remains unchanged, coinciding with what is observed with the brown curve.

However, addition of a lower concentration of τ-peptide, corresponding to approximately half of 14-3-3τ being bound to τ-peptide, shows a shift towards the right. At the lower peptide concentration half of 14-3-3τ is expected to be bound. This means that the other half, roughly 375 nM 14-3-3τ, is free to bind to α-synuclein. Based on this, we would still expect an effect of 14-3-3τ on the multimerization of α-syn, only smaller than compared to 750 nM free 14-3-3τ. This difference in effect would result in a binding curve in between the observed red and brown curves. Yet, the curve is shifted more to the right, indicating the opposite effect is happening compared to adding only 14-3-3τ. This same effect was observed in experiment 1 and suggests that the presence of τ-peptide interferes with α-syn multimerization by possibly interacting with α-syn itself.

However, combining the results from experiment 1 and 2, they do not coincide. If τ-peptide would indeed interfere α-syn multimerization by interacting with it, this effect would also have to be visible after adding the high concentration of τ-peptide of 4.5 μM. With such high concentration of τ-peptide, there should be plenty free τ-peptide to interact with α-syn which would then result in the same right shift of the curve. Unfortunately, the results measuring the possible interaction between τ-peptide and α-syn deemed inconclusive (see *Interaction between τ-Peptide and α-Synuclein*), making it difficult to assess the effect of τ-peptide on the multimerization curve. This interaction should thus be further investigated.

Experiment 3

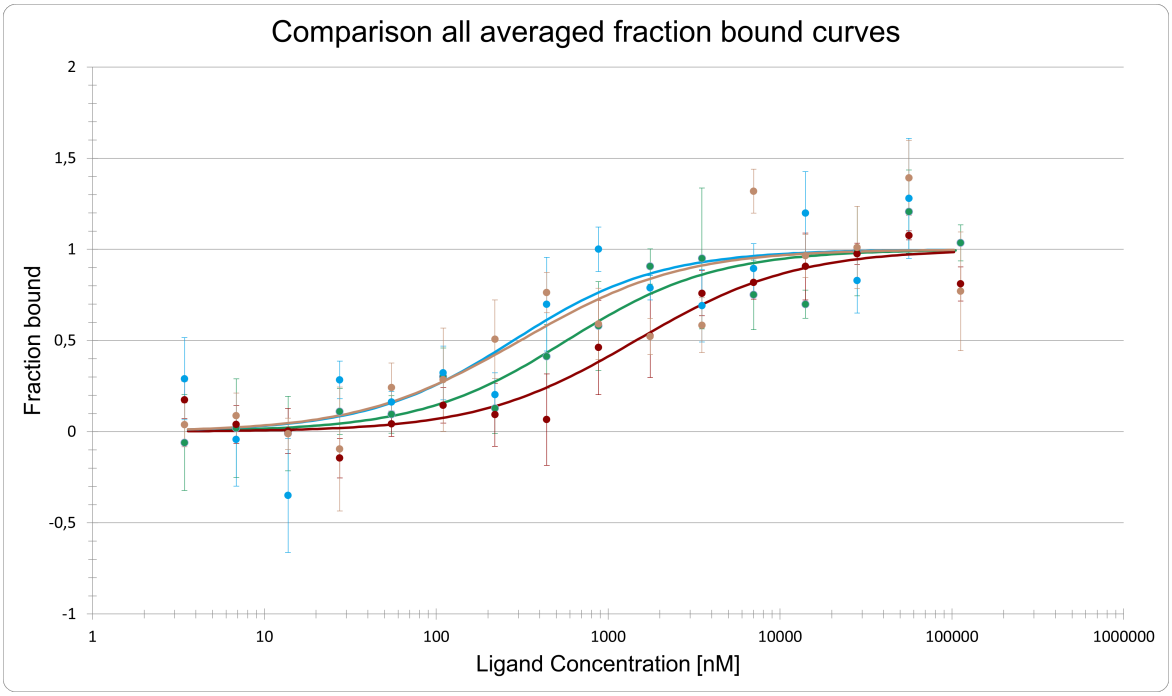

Figure 18: Average fraction bound curves of different protein interaction measurements. The green curve shows α-syn multimerization (fitted K_D = 564.4 ± 397.0 nM). The red curve shows α-syn multimerization in presence of 1.5 μM 14-3-3τ (fitted K_D = 1632.9 ± 944.4 nM). The blue curve shows α-syn multimerization in presence of 1.5 μM 14-3-3τ and 950 nM τ-peptide (fitted K_D = 265.2 ± 260.6 nM). The brown curve shows α-syn multimerization in presence of 1.5 μM 14-3-3τ and 5.2 μM τ-peptide (fitted K_D = 346.7 ± 310.3 nM). Target concentration α-synAF488 was 50 nM. Ligand concentration ranged from 112.5 μM down to 3.4 nM. Curves are average of the fraction bound curves at 20%, 40%, 60% and 80% MST power. Ligand concentrations are given in nM on a logarithmic x-axis. Measurement done at 23 °C. Error bars correspond to the standard deviation from the averaged four MST power measurements.

Measurements with higher concentration 14-3-3τ revealed contradicting results compared to the results discussed above. At a 14-3-3τ concentration of 1.5 μM the fraction bound curve is shifted towards the right as depicted by the red curve (Figure 17). An explanation could be that the high concentration of 14-3-3τ causes more than one 14-3-3τ dimer to bind to the α-synuclein multimers. Upon binding of multiple dimers, the multimers might dissociate causing the equilibrium to shift towards the formation of monomers which leads to a shifted binding curve to the right. When τ-peptide is added, an opposite shift is shown for both concentrations with no significant difference between the two peptide concentrations. Though there is no difference in effect between the two added peptide concentrations, the observation that the addition of τ-peptide again seems to counteract the addition of 14-3-3τ alone, indicates competition between the τ-peptide and α-synuclein at the amphipathic groove of 14-3-3τ.

Though it has been observed that the τ-peptide appears to counteract the effect of 14-3-3τ on the multimerization of α-synuclein, other effects were also observed challenging the validity of this conclusion. At higher τ-peptide concentration, a shift to the left is depicted (Figure 18, brown curve). It could be that the τ-peptide is not fully

bound to 14-3-3τ but also to the surface of the capillary or to α-synuclein, as was seen in the interaction measurement between τ-peptide and α-synuclein. This would result in more free 14-3-3τ which can bind to the multimers, resulting in the observed shift to the left for higher τ-peptide concentration. Though this could explain the shifts towards the left for these curves, these observations do not coincide with the opposite right shift that is seen for the red curve after adding only 14-3-3τ.

In summary, the MST data shows that α-syn does indeed form multimers with good reproducibility along different measurements. Additionally, the competition assays using 750 nM and 1.5 μM 14-3-3τ show an effect of 14-3-3τ on the multimerization of α-synuclein, suggesting possible interaction between 14-3-3τ and α-syn multimers. They also show that addition of various concentrations of τ-peptide seemingly nullifies or counteracts the effect of 14-3-3τ on said multimerization, indicating competition between τ-peptide and α-syn for binding in the amphipathic groove.

However, the above mentioned competition experiments display contradicting results between the different concentrations of added 14-3-3τ, as well as the different τ-peptide concentrations. These various, conflicting results complicate formulation of a cohesive and complete conclusion. This variability in results suggests it would be interesting to further investigate the complexity of the 14-3-3τ/α-syn interaction, by looking at reaction stochiometry or the possibility of different 14-3-3 binding modes being used upon interaction.

Finally, in this research microscale thermophoresis was used to conduct all protein interaction measurements. While MST forms a great method to investigate molecular interactions and deriving binding affinities, it also has its limitations. The instrument uses blue and/or green excitation, slightly limiting the use of certain fluorescent dyes for labeling as seen with the ATTO 647N dye for 14-3-3τ labeling (see *Investigating Different Target Behaviour upon Interaction with α-Synuclein Ligand*). Furthermore, variables such as LED power, MST power and temperature should be considered carefully when setting up an experiment. Increasing MST powers increase the chance of unfolding and aggregation events of the target sample. Increasing the LED power increases the target's initial fluorescence, making it possible to perform measurements even at low dye labeling efficiencies, but could also increase the photobleaching effect as mentioned before.

5 Conclusion

The initial goal of this research was to gain more information on the interaction between 14-3-3 and α-synuclein, particularly information regarding 14-3-3τ's binding site used interaction with α-synuclein. It was hypothesized that there is indeed interaction between the two proteins and that 14-3-3 affects α-synuclein aggregation by binding it in its amphipathic groove.

α-synuclein was found to multimerize with a fitted K_D of 564.4 $\pm$ 397.0 nM. MST measurements with α-synuclein and 14-3-3τ revealed an effect of 14-3-3τ on the multimerization of α-synuclein.

While a definitive conclusion on the binding sites of 14-3-3τ upon interaction with α-synuclein has not been found, the competition assays have shown that the τ-peptide seems to counteract the effect of 14-3-3τ on α-syn multimerization, indicating that the amphipathic groove may indeed play a role in the interaction between 14-3-3τ and α-syn. Though, the obtained results of the different competition experiments were highly contradictory, implying the need for further research into the 14-3-3τ/α-syn interaction.

Furthermore, this research has gained more information on the many effects that can occur during MST. It was found that target labeling, among other effects such as MST power, temperature and sample centrifuging have an effect on protein interactions and the quality of measurements in MST. It has provided deeper insight on the behaviour of 14-3-3τ in MST and its sensitivity for temperature induced effects, labeling and sample homogeneity. Experimental optimization revealed that 14-3-3τ labeled with ATTO 647N is unsuitable for use in MST and different dyes (e.g. Alexa Fluor 568) should be used for target labeling.

References

[1] David T. Dextera and Peter Jenner. *Parkinson disease: From pathology to molecular disease mechanisms*. Sept. 2013. DOI: 10.1016/j.freeradbiomed.2013.01.018.

[2] Yvette C. Wong and Dimitri Krainc. "α-synuclein toxicity in neurodegeneration: Mechanism and therapeutic strategies". In: *Nature Medicine* 23.2 (2017), pp. 1–13. ISSN: 1546170X. DOI: 10.1038/nm.4269.

[3] Matthew J. Benskey, Ruth G. Perez, and Fredric P. Manfredsson. *The contribution of alpha synuclein to neuronal survival and function - Implications for Parkinson's disease*. May 2016. DOI: 10.1111/jnc.13570. URL: https://onlinelibrary-wiley-com.ezproxy2.utwente.nl/doi/full/10.1111/jnc.13570%20https://onlinelibrary-wiley-com.ezproxy2.utwente.nl/doi/abs/10.1111/jnc.13570%20https://onlinelibrary-wiley-com.ezproxy2.utwente.nl/doi/10.1111/jnc.13570.

[4] Jessika C. Bridi and Frank Hirth. *Mechanisms of α-Synuclein induced synaptopathy in parkinson's disease*. Feb. 2018. DOI: 10.3389/fnins.2018.00080.

[5] Ronit Sharon et al. "The formation of highly soluble oligomers of α-synuclein is regulated by fatty acids and enhanced in Parkinson's disease". In: *Neuron* 37.4 (Feb. 2003), pp. 583–595. ISSN: 08966273. DOI: 10.1016/S0896-6273(03)00024-2.

[6] Wei Wang et al. "A soluble α-synuclein construct forms a dynamic tetramer". In: *Proceedings of the National Academy of Sciences of the United States of America* 108.43 (Oct. 2011), pp. 17797–17802. ISSN: 00278424. DOI: 10.1073/pnas.1113260108. URL: www.pnas.org/cgi/doi/10.1073/pnas.1113260108.

[7] E. Giusto et al. "Pathways to Parkinson's disease: a spotlight on 14-3-3 proteins". In: *npj Parkinson's Disease* 7.1 (2021). ISSN: 23738057. DOI: 10.1038/s41531-021-00230-6. URL: http://dx.doi.org/10.1038/s41531-021-00230-6.

[8] Nicoletta Plotegher et al. "The chaperone-like protein 14-3-3η interacts with human α-synuclein aggregation intermediates rerouting the amyloidogenic pathway and reducing α-synuclein cellular toxicity". In: *Human Molecular Genetics* 23.21 (Nov. 2014), pp. 5615–5629. ISSN: 0964-6906. DOI: 10.1093/HMG/DDU275. URL: https://academic-oup-com.ezproxy2.utwente.nl/hmg/article/23/21/5615/2900985.

[9] Rachel Underwood et al. "14-3-3 mitigates alpha-synuclein aggregation and toxicity in the in vivo preformed fibril model". In: *Acta Neuropathologica Communications* 9.1 (Dec. 2021), pp. 1–16. ISSN: 20515960. DOI: 10.1186/S40478-020-01110-5/FIGURES/5. URL: https://actaneurocomms.biomedcentral.com/articles/10.1186/s40478-020-01110-5.

[10] Bing Wang et al. "14-3-3 proteins reduce cell-to-cell transfer and propagation of pathogenic α-synuclein". In: *Journal of Neuroscience* 38.38 (Sept. 2018), pp. 8211–8232. ISSN: 15292401. DOI: 10.1523/JNEUROSCI.1134-18.2018. URL: https://www.jneurosci.org/content/38/38/8211%20https://www.jneurosci.org/content/38/38/8211.abstract.

[11] Moran Jerabek-Willemsen et al. “MicroScale Thermophoresis: Interaction analysis and beyond”. In: *Journal of Molecular Structure* 1077 (2014), pp. 101–113. ISSN: 00222860. DOI: 10.1016/j.molstruc.2014.03.009. URL: http://dx.doi.org/10.1016/j.molstruc.2014.03.009.

[12] Susanne A.I. Seidel et al. “Microscale thermophoresis quantifies biomolecular interactions under previously challenging conditions”. In: *Methods* 59.3 (Mar. 2013), pp. 301–315. ISSN: 10959130. DOI: 10.1016/J.YMETH.2012.12.005.

[13] Moran Jerabek-Willemsen et al. *Molecular interaction studies using microscale thermophoresis*. Aug. 2011. DOI: 10.1089/adt.2011.0380. URL: /pmc/articles/PMC3148787/%20/pmc/articles/PMC3148787/?report=abstract%20https://www.ncbi.nlm.nih.gov/pmc/articles/PMC3148787/.

[14] Arthur Sedivy. “Standard operating procedure for NanoTemper Monolith measurements”. In: *European Biophysics Journal* 50.3-4 (2021), pp. 381–387. ISSN: 14321017. DOI: 10.1007/s00249-021-01534-4. URL: https://doi.org/10.1007/s00249-021-01534-4.

[15] NanoTemper Technologies GmbH. *Kd*. URL: https://nanotempertech.com/nanopedia/kd/.

[16] NanoTemper Technologies GmbH. *EC50*. URL: https://nanotempertech.com/nanopedia/ec50/.

[17] Julie M. Rainard, George C. Pandarakalam, and Stuart P. McElroy. *Using Microscale Thermophoresis to Characterize Hits from High-Throughput Screening: A European Lead Factory Perspective*. Mar. 2018. DOI: 10.1177/2472555217744728.

[18] Blanca López-Méndez et al. “Microscale Thermophoresis and additional effects measured in NanoTemper Monolith instruments”. In: *European Biophysics Journal* 50.3-4 (2021), pp. 653–660. ISSN: 14321017. DOI: 10.1007/s00249-021-01529-1. URL: https://doi.org/10.1007/s00249-021-01529-1.

[19] NanoTemper Technologies GmbH. *Photobleaching*. URL: https://nanotempertech.com/nanopedia/photobleaching/%20https://nanotempertech.com/nanopedia/fluorophores/.

[20] Thermo Fisher Scientific. *Protein Labeling Kits For Alexa Fluor™, Pacific Blue™, Fluorescein-EX, and Oregon Green™ 488)*. 2021.

[21] NanoTemper Technologies GmbH. “MST Starting Guide – Monolith NT.115”. In: (), pp. 1–13.

[22] *Fluorescein (FITC) | Thermo Fisher Scientific - NL*. URL: https://www.thermofisher.com/nl/en/home/life-science/cell-analysis/fluorophores/fluorescein.html.

[23] ExPASy. *ProtParam*. URL: https://web.expasy.org/cgi-bin/protparam/protparam1?P27348@noft@.

[24] ATTO-TEC GmbH. “Product Information : ATTO 647N, Cat No.: AD 647N-3”. In: (2013), p. 2.

Appendix A

Protein	ϵ_{280} **(M^{-1} cm^{-1})**
α-synuclein	5600
14-3-3τ	26,060

Table 1: Properties of the unlabeled proteins used. ϵ_{280} = extinction coefficient of the protein at 280 nm [23].

Dye	λ_{max} **(nm)**	ϵ_{dye} **(M^{-1} cm^{-1})**	**CF**
Alexa Fluor 488	494	71,000	0.11
Alexa Fluor 568	577	91,300	0.46
ATTO 647N	646	$1.5{\cdot}10^5$	0.03

Table 2: Properties of the different dyes used for protein labeling [20, 24]. λ_{max} = wavelength maximum of the dye. ϵ_{dye} = extinction coefficient of the dye at its maximum wavelength λ_{max}. CF = correction factor for the absorbance measured at 280 nm.

Appendix B

	α-synuclein multimerization	**14-3-3τ and α-syn**	**14-3-3τ and τ-peptide**	**τ-peptide and α-syn**
Target concentration	α-synAF488 50 nM	14-3-3τ AF568 50 nM	14-3-3τ AF568 50 nM	τ-FITC peptide 200 nM
Ligand concentration range	α-synWT 112.5 μM - 3.4 nM	α-synWT 112.5 μM - 3.4 nM	τ-peptide 10 μM - 0.30 nM	α-synWT 110 μM - 3.4 nM

Table 3: Measurement specifics of the different direct interaction measurements discussed in *Materials and Methods*.